Electronic Supplementary Material (ESI) for CrystEngComm.

Supporting Information

Pillared-bilayer zinc(II)–organic laminae: pore modification and selective gas adsorption

Li-Wei Lee,[ab] Sheng-Han Lo,[a] Tzuoo-Tsair Luo,[a] Gene-Hsiang Lee,[d] Shie-Ming Peng,[d] Yen-Hsiang Liu,*[c] Sheng-Long Lee*[b] and Kuang-Lieh Lu*[a]

[a]Institute of Chemistry, Academia Sinica, Taipei 115, Taiwan
[b]Institute of Materials Science and Engineering, National Central University, Taoyuan 320, Taiwan
[c]Department of Chemistry, Fu Jen Catholic University, New Taipei City 242, Taiwan
[d]Department of Chemistry, National Taiwan University, Taipei 107, Taiwan

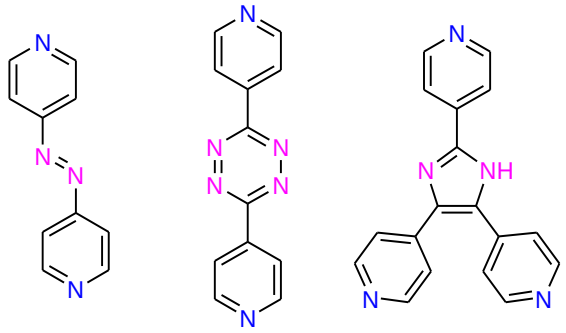

Scheme S1 Selected ligands that act as a pillar in the target frameworks.

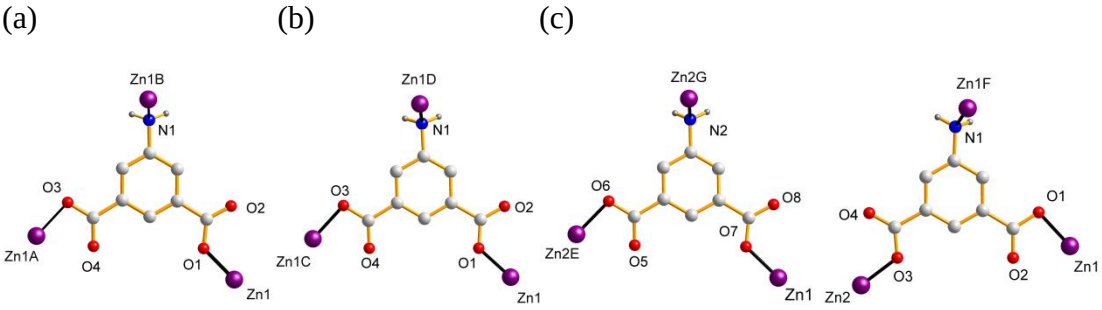

Fig. S1 The coordination modes of the aip^{2-} ligand in **1** (a), **2** (**b**), and **3** (c).[symmetry code: **1**, (A) x, -y+3/2, z-1/2; (B) x, -y+1/2, z-1/2; **2**, (C) -x+1, -y, -z+1; (D) x, -y+3/2, z+1/2; **3**, (E) x-1, y, z; (F) x, y+1, z; (G) x-1, y-1, z.]

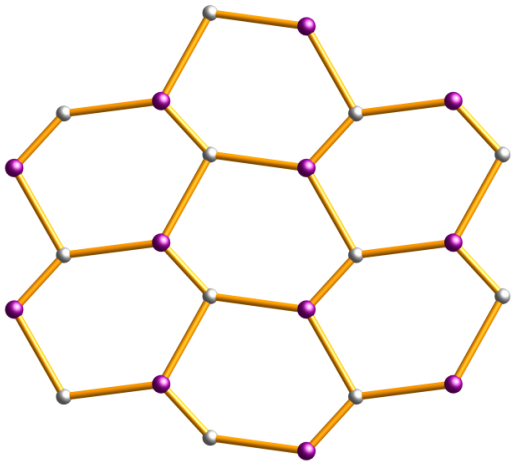

Fig. S2 A graphical representation of the (6,3)-net topology in **1**–**3**. (purple: Zn atoms; gray: the geometry centers of the aip^{2-} rings).

(a)

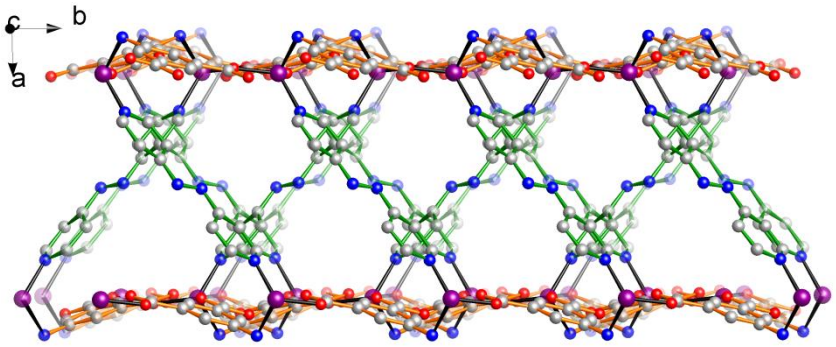

(b)

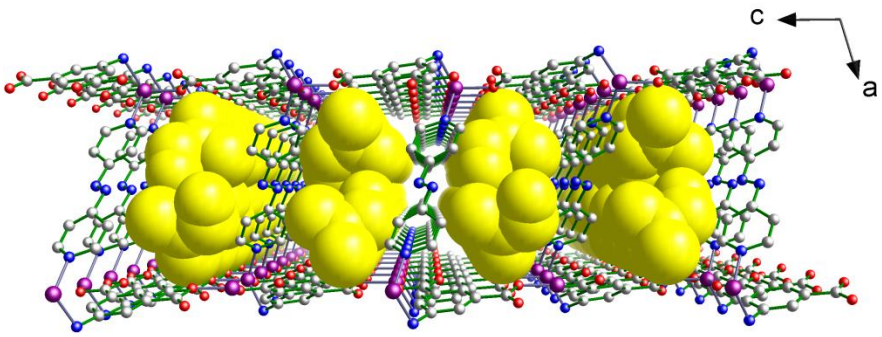

(c)

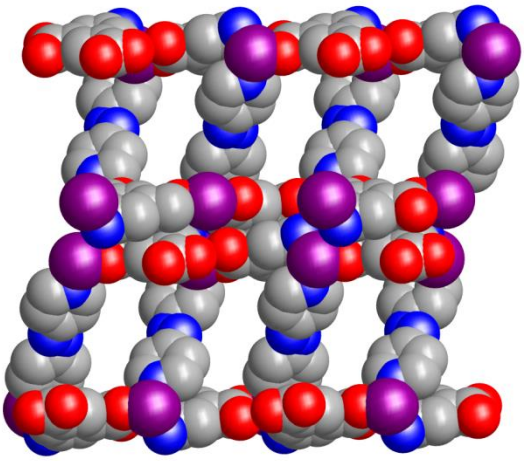

Fig. S3 (a) The smaller channels of **1** were observed along the *c* axis. (b) A perspective view of the DMF (yellow) molecules within the 1D channels. (c) Superimposed space-filling representation of **1** showing one-dimensional channels.

(a)

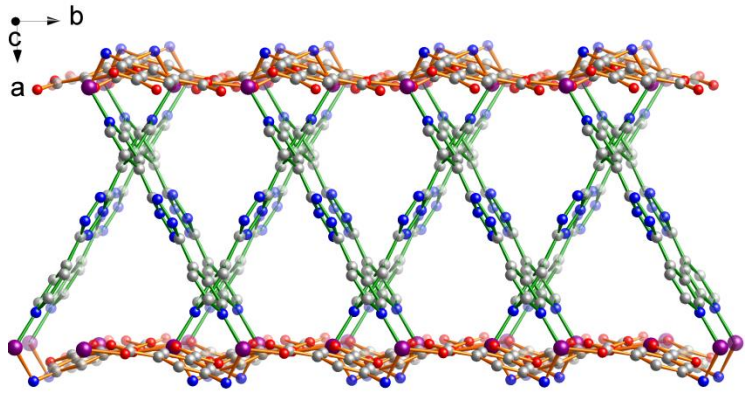

(b)

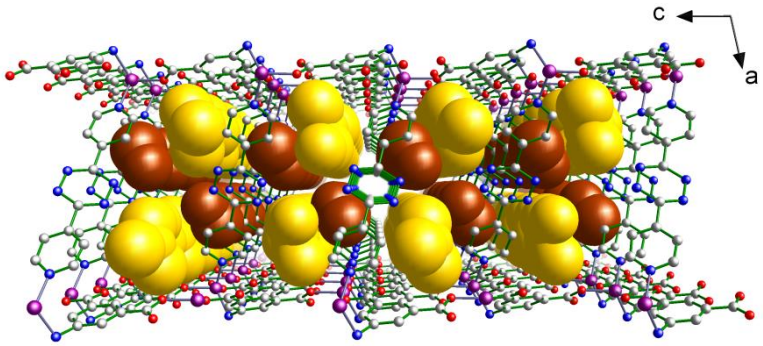

(b)

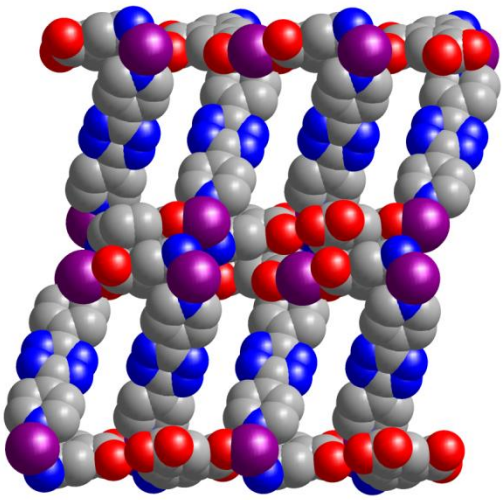

Fig. S4 (a) The smaller channels of **2** were observed along the *c* axis. (b) A perspective view of the DMF (yellow) and MeOH (brown) molecules within the 1D channels. (c) Superimposed space-filling representation of **2** showing one-dimensional channels.

(a)

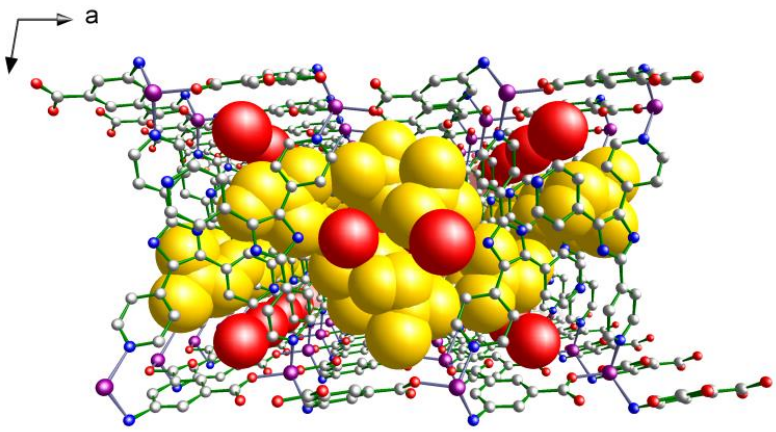

(b)

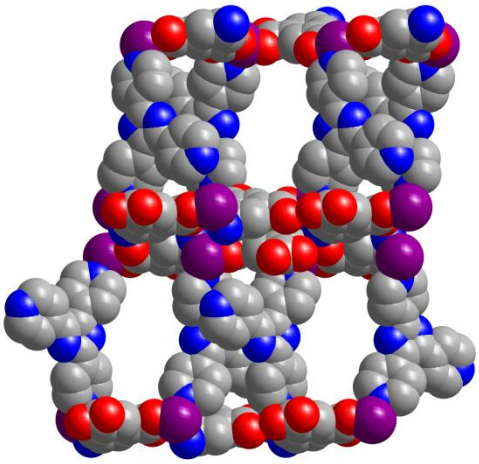

Fig. S5 (a) A perspective view of the DMF (yellow) and H_2O (red) molecules within the 1D channels. (b) Superimposed space-filling representation of **3** showing one-dimensional channels.

(a)

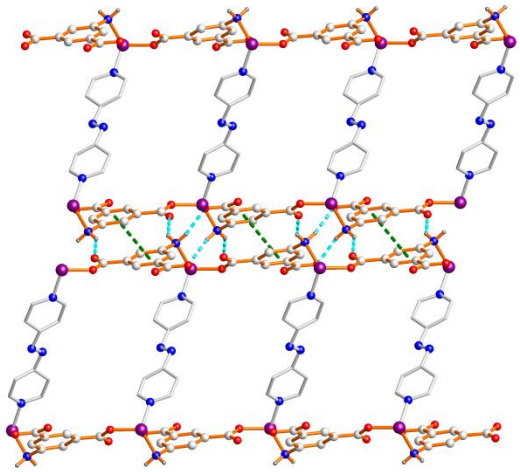

(b)

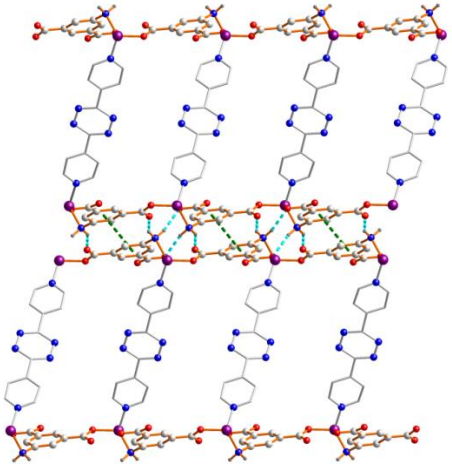

(c)

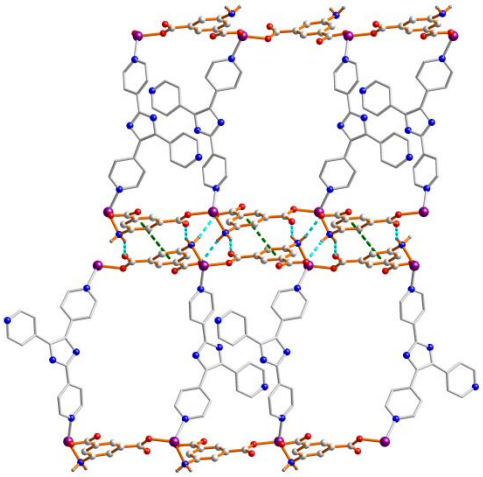

Fig. S6 A view of hydrogen bonding (sky blue dotted lines) and π–π stacking (green dotted lines) interactions between the 2D layers in **1** (a), **2** (b), and **3** (c).

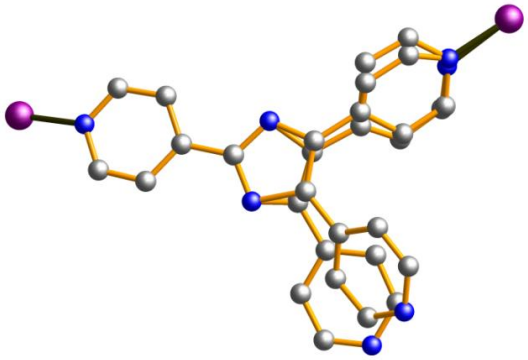

Fig. S7 View of the disordered tpim ligand and uncoordinated pyridyl group in **3**.

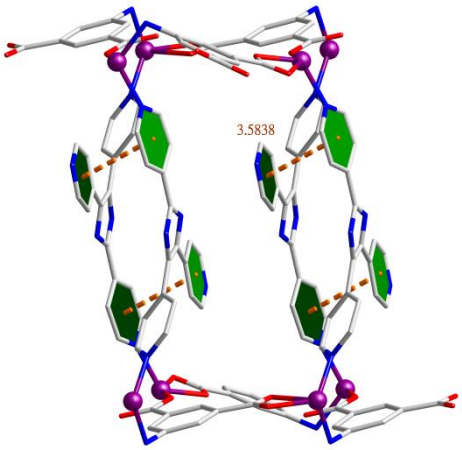

Fig. S8 The 2-D pillared-bilayer network of compound **3** extended by π–π stacking interactions from the pyridyl and other aromatic rings.

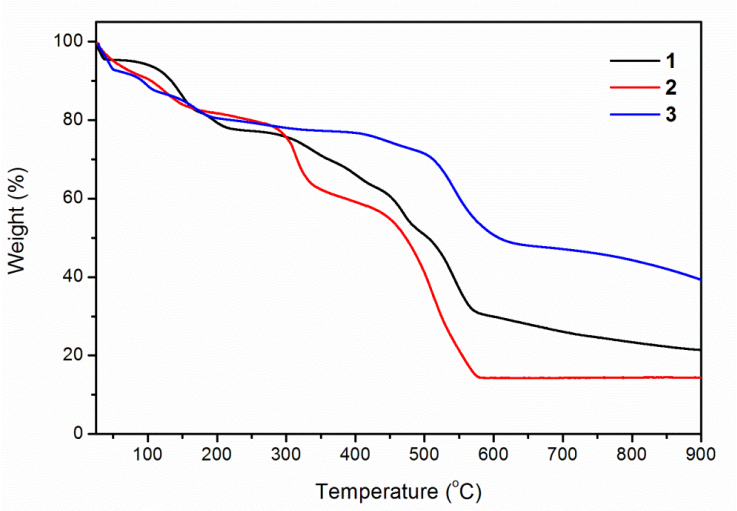

Fig. S9 Thermogravimetric (TG) diagrams for **1**–**3**.

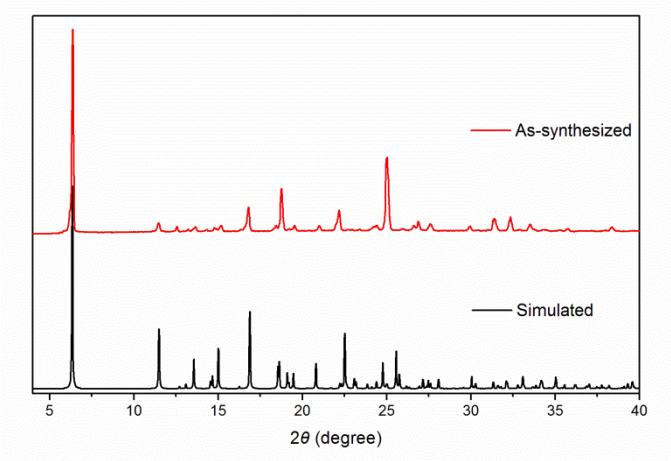

Fig. S10 Simulated PXRD patterns from the crystal structure (black) and the as-synthesized (red) sample for compound **1**.

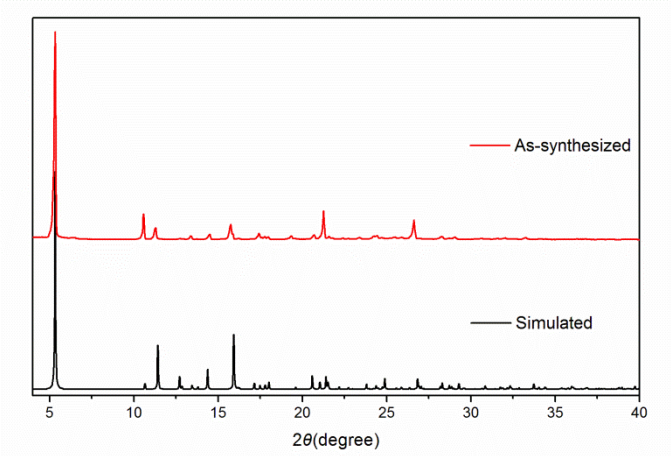

Fig. S11 Simulated PXRD patterns from the crystal structure (black) and the as-synthesized (red) sample for compound **2**.

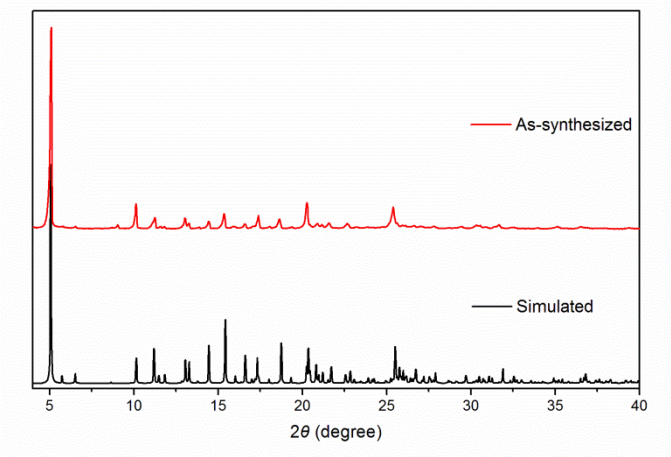

Fig. S12 Simulated PXRD patterns from the crystal structure (black) and the as-synthesized (red) sample for compound **3**.

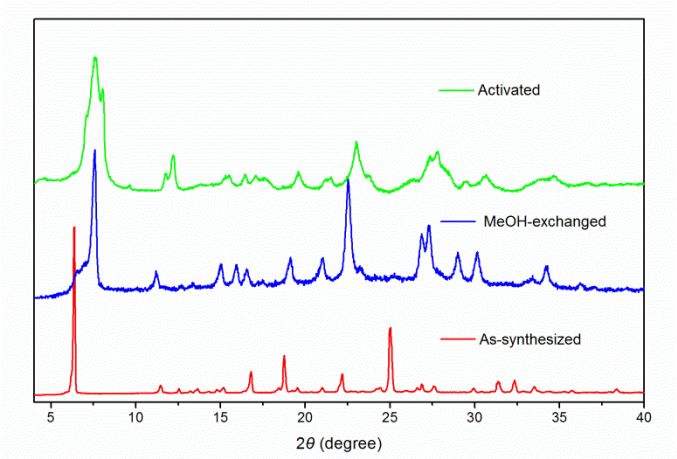

Fig. S13 Simulated PXRD patterns from the as-synthesized (red), MeOH-exchanged (blue) and activated sample (green) for compound **1**.

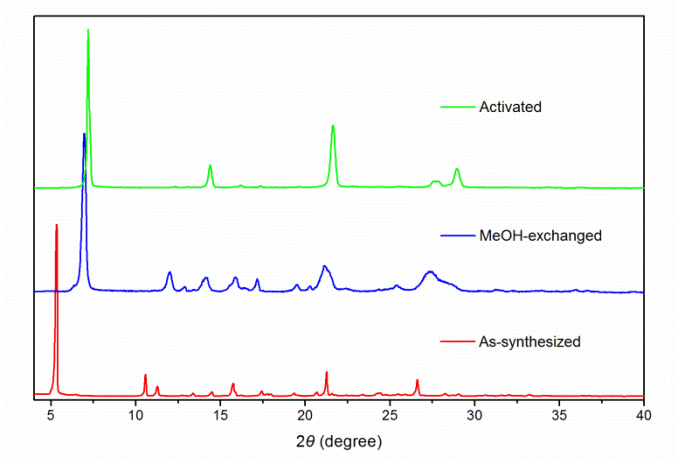

Fig. S14 Simulated PXRD patterns from the as-synthesized (red), MeOH-exchanged (blue) and activated sample (green) for compound **2**.

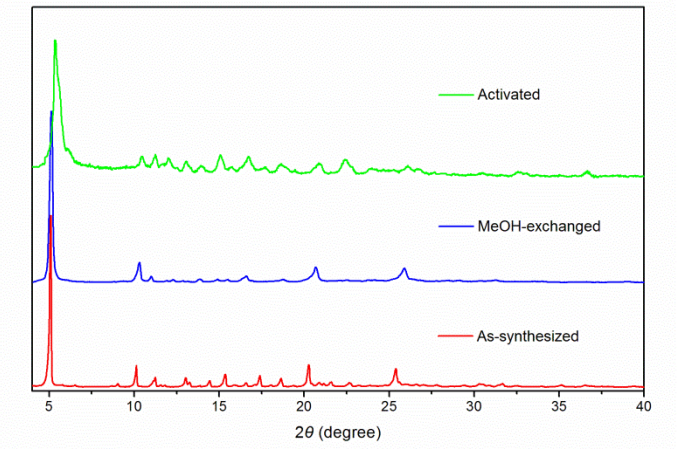

Fig. S15 Simulated PXRD patterns from the as-synthesized (red), MeOH-exchanged (blue) and activated sample (green) for compound **3**.

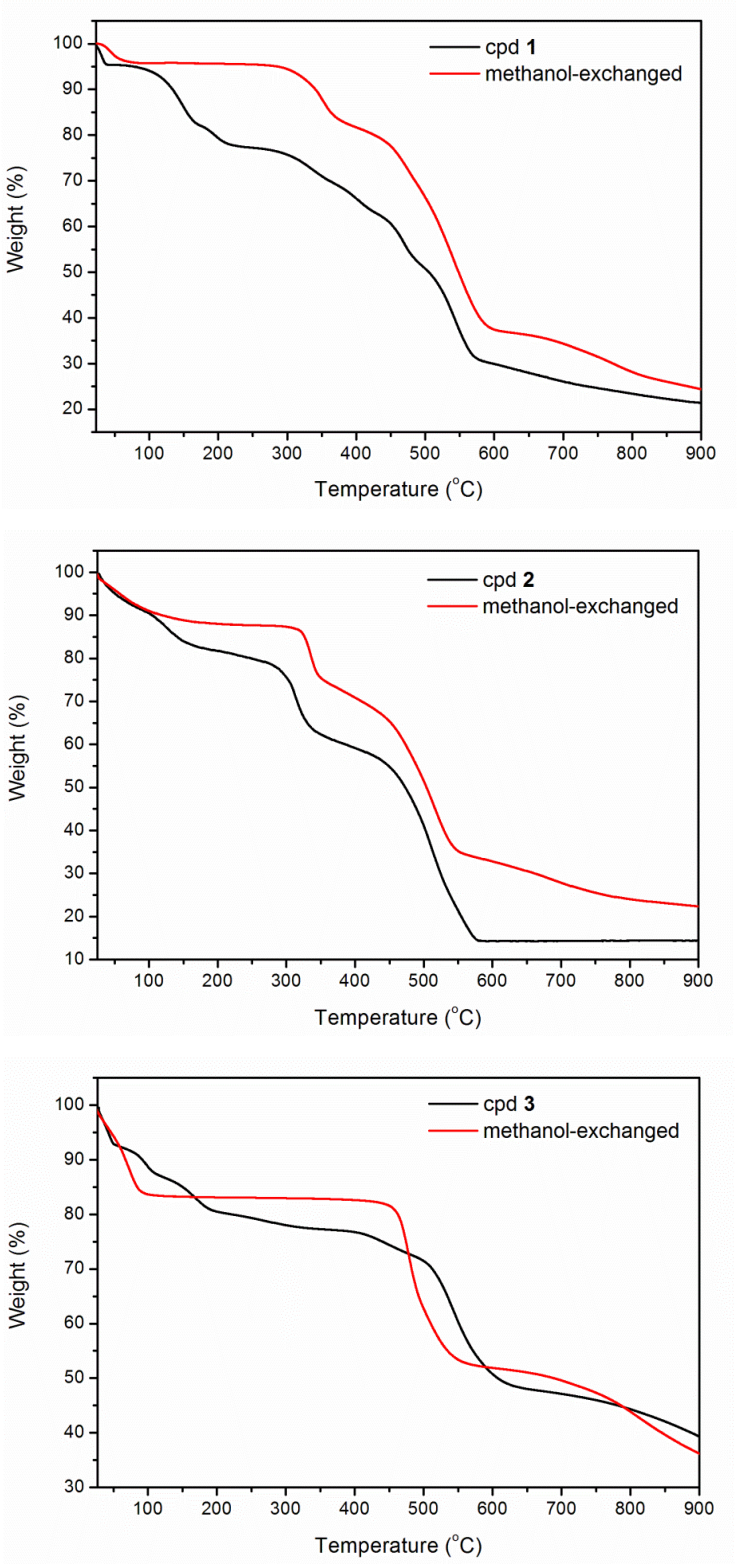

Fig. S16 Thermogravimetric (TG) diagrams for the as-synthesized (black) and the MeOH-exchanged (red) sample in **1–3**.

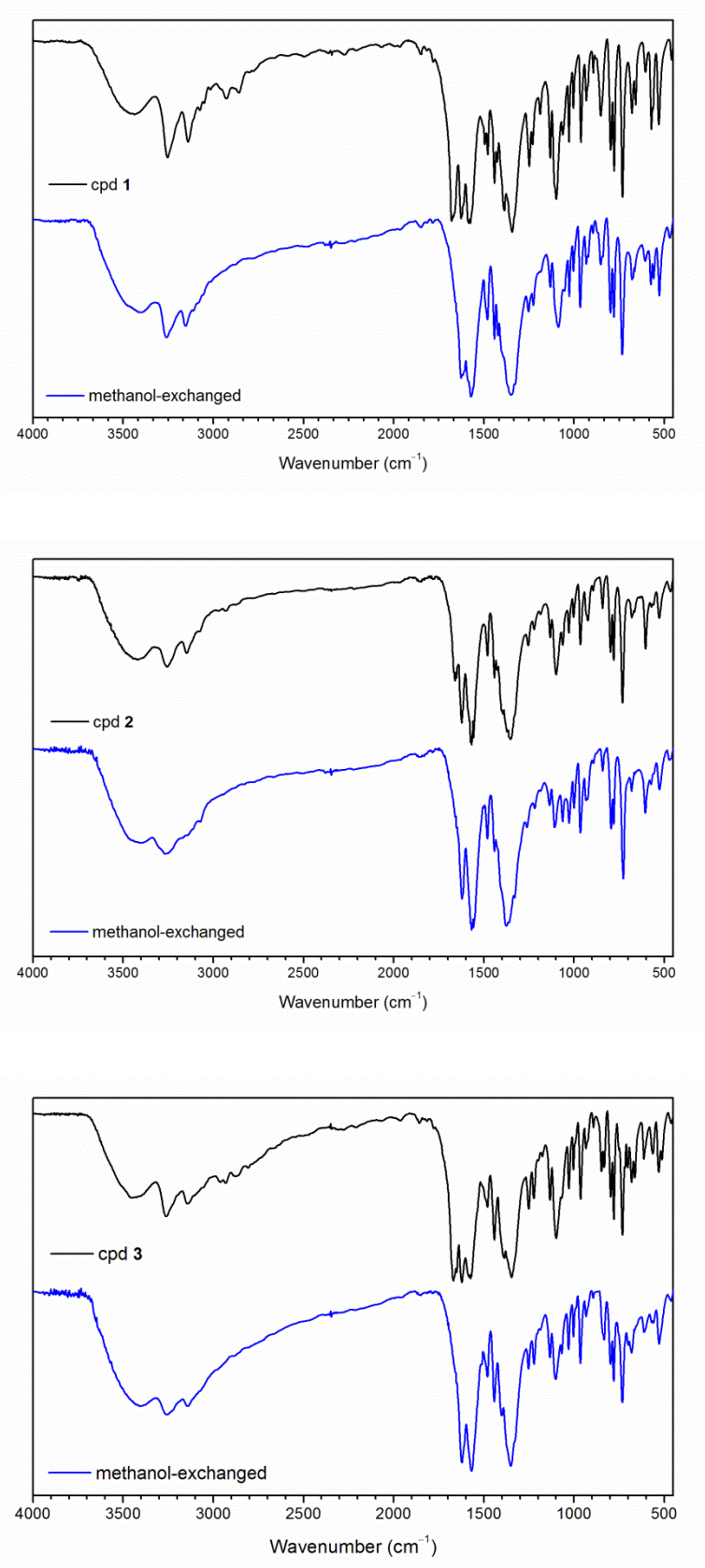

Fig. S17 IR spectra of **1**–**3**.

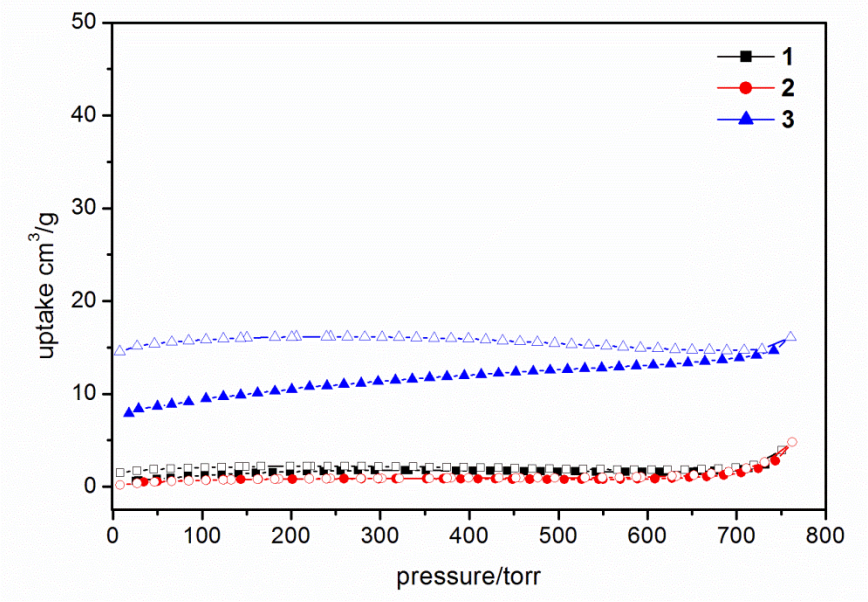

Fig. S18 N_2 adsorption isotherms of **1**–**3** at 77 K.

Estimation of the isosteric heats of gas adsorption

A virial-type expression comprising the temperature-independent parameters a_i and b_i was employed to calculate the enthalpies of adsorption for CO_2 (at 273 K and 298 K) on **1**–**3**. In each case, the data were fitted using the equation 1:

$$\ln P = \ln N + 1/\mathrm{T} \sum_{i=0}^{m} a_i N^i + \sum_{i=0}^{n} b_i N^i \qquad (1)$$

Here, P is the pressure expressed in torr, N is the amount adsorbed in mmol/g, T is the temperature in K, a_i and b_i are virial coefficients, and m, n represent the number of coefficients required to adequately describe the isotherms (m and n were gradually increased until the contribution of extra added a and b coefficients was deemed to be statistically in insignificant towards the overall fit, and the average value of the squared deviations from the experimental values was minimized). The values of the virial coefficients a_0 through a_m were then used to calculate the enthalpies heat of adsorption using the following expression 2.

$$Q_{st} = -R \sum_{i=0}^{\mathrm{m}} a_i N^i \qquad (2)$$

Q_{st} is the coverage-dependent isosteric heat of adsorption and R is the universal gas constant.

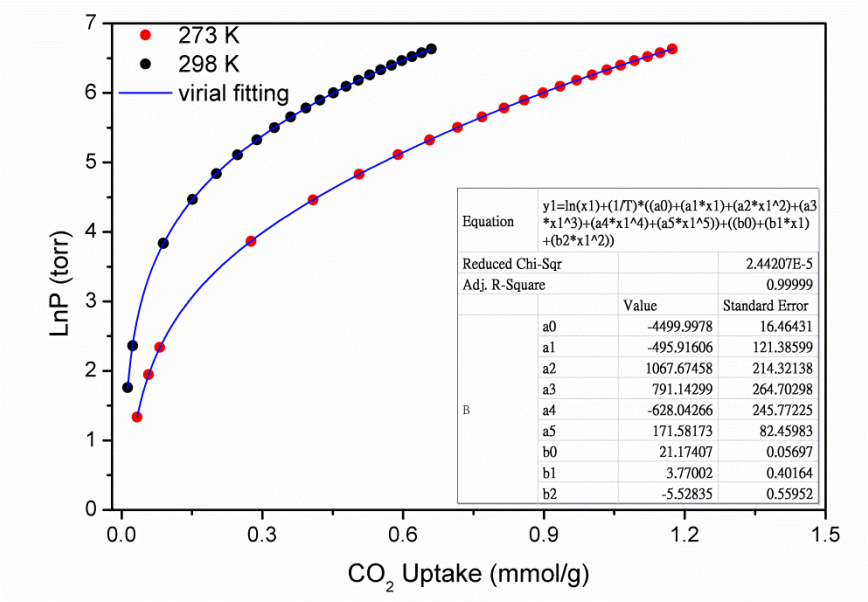

Fig. S19 The CO_2 adsorption isotherms at 273 K (red) and 298 K (black) for **1** fitting by virial method.

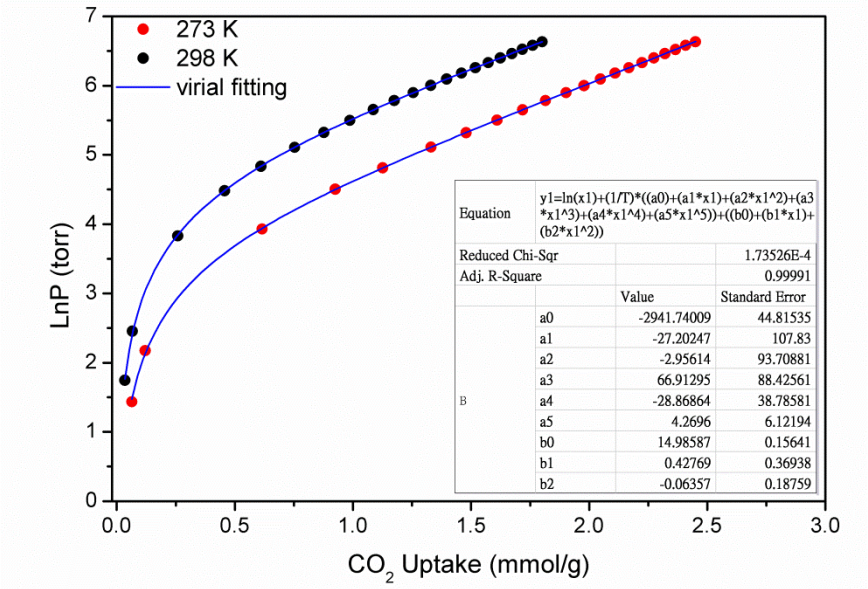

Fig. S20 The CO_2 adsorption isotherms at 273 K (red) and 298 K (black) for **2** fitting by virial method.

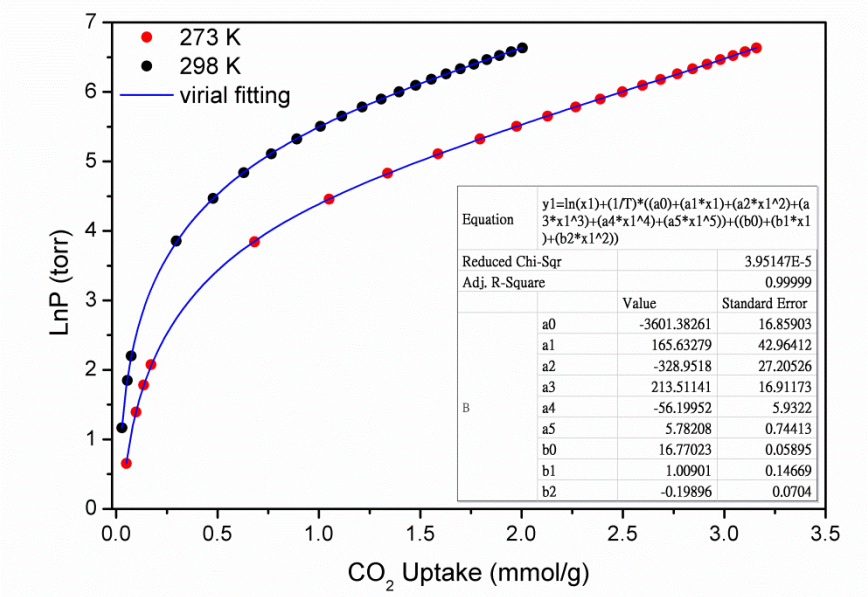

Fig. S21 The CO_2 adsorption isotherms at 273 K (red) and 298 K (black) for **3** fitting by virial method.